Solar-Terrestrial Physics. 2025, vol. 11, iss. 3, pp. 125–134. DOI: 10.12737/stp-113202515. © 2025 A.V. Bogomolov, V.V. Bogomolov, A.F. Iyudin, V.V. Kalegaev, I.N. Myagkova, V.I. Osedlo, S.I. Svertilov, I.V. Yashin. Published by INFRA-M Academic Publishing House

DOI: 10.12737/stp-113202515

Received February 28, 2025
Accepted May 12, 2025

MONITORING OF SPACE WEATHER EFFECTS WITH SOZVEZDIE-270 NANOSATELLITE CONSTELLATION OF MOSCOW UNIVERSITY

A.V. Bogomolov
Lomonosov Moscow State University, Skobeltsyn Institute of Nuclear Physics, Moscow, Russia, aabboogg@srd.sinp.msu.ru

V.V. Bogomolov
Lomonosov Moscow State University, Skobeltsyn Institute of Nuclear Physics, Moscow, Russia, bogovit@rambler.ru
Lomonosov Moscow State University, Faculty of Physics, Moscow, Russia

A.F. Iyudin
Lomonosov Moscow State University, Skobeltsyn Institute of Nuclear Physics, Moscow, Russia, aiyudin@srd.sinp.msu.ru

V.V. Kalegaev
Lomonosov Moscow State University, Skobeltsyn Institute of Nuclear Physics, Moscow, Russia, klg@dec1.sinp.msu.ru
Lomonosov Moscow State University, Faculty of Physics, Moscow, Russia

I.N. Myagkova
Lomonosov Moscow State University, Skobeltsyn Institute of Nuclear Physics, Moscow, Russia, irina@srd.sinp.msu.ru

V.I. Osedlo
Lomonosov Moscow State University, Skobeltsyn Institute of Nuclear Physics, Moscow, Russia, osedlo@mail.ru

S.I. Svertilov
Lomonosov Moscow State University, Skobeltsyn Institute of Nuclear Physics, Moscow, Russia, sis@coronas.ru
Lomonosov Moscow State University, Faculty of Physics, Moscow, Russia

I.V. Yashin
Lomonosov Moscow State University, Skobeltsyn Institute of Nuclear Physics, Moscow, Russia, ivn@eas.sinp.msu.ru

Abstract. The space project Sozvezdie-270 of Moscow University is in progress now. It involves the deployment of a CubeSat nanosatellites constellation. To the present, 20 satellites have been launched, 9 of them continue to function in near-Earth orbit; one more will be launched in the near future. Instruments were developed specifically for the experiments on board small spacecraft of the CubeSat format, which provide measurements of fluxes and spectra of charged particles, primarily electrons of relativistic and sub-relativistic energies, as well as gamma quanta. Along with the space constellation, a network of ground receiving stations is also being created. A multi-satellite constellation gives a number of advantages in studying dynamic processes in near-Earth space. In particular, it makes possible to carry out simultaneous measurements of charged particle fluxes with instruments of the same type at different points in near-Earth space. Such measurements provide unique information about the flux of sub-relativistic electrons, including variations due to precipitation of electrons, which is of great importance for understanding the mechanisms of acceleration and losses of trapped and quasi-trapped electrons in Earth's radiation belts (ERB).

We discuss various recent space weather manifestations associated with increased solar flare activity. Among such effects is the filling of the polar caps with particles of solar cosmic rays, dynamic processes in outer ERB during magnetic storms, rapid variations in electron fluxes due to precipitation.

Keywords: space weather, Earth's radiation belts, solar cosmic rays, nanosatellites, CubeSat.

INTRODUCTION

Space weather is a relatively young branch of physics, which studies extremely variable conditions in near-Earth space (NES). These variations are caused by active processes on the Sun, conditions in the interplanetary medium (variations in interplanetary magnetic field (IMF) and solar wind (SW) parameters) and in the magnetosphere—ionosphere—thermosphere system, as well as their influence on Earth and human activity. Adverse changes in NES can reduce the efficiency and reliability of spacecraft and ground-based systems, which, in turn, can lead to heavy losses due to problems in operating communication systems, navigation, power systems, and reconnaissance satellites [Baker, 2001; Belov et al., 2004; Iucci et al., 2005; Romanova et al., 2005; Potapov et al., 2016; Novikov, Voronina, 2021]. That is why space weather has become one of the fastest-growing areas of research over the past few decades [Daglis,

2001; Cole, 2003; Schrijver et al., 2015; McGranaghan et al., 2021]. Nowadays, space weather forecast centers have been established by several national governments and research institutes (e.g., [Wei et al., 2003; Lundstedt, 2006; Wilkinson, 2009]).

One of the main space weather effects includes variations in energetic charged particle fluxes in various NES regions [Kudela, 2013]. At the same time, variations in particle and quantum fluxes recorded by instruments can be caused either by a satellite crossing a compact region with increased particle density (so-called spatial effects) or by an increase (or decrease) in intensity (temporal effects). In turn, both spatial and temporal effects can be related to acceleration of particles and their precipitation from the regions of trapped radiation — Earth's radiation belts (ERB), as well as to penetration of particles accelerated in solar flares into the magnetosphere, i.e. the so-called solar cosmic rays (SCRs) [Dorman, Miroshnichenko, 1968].

Experimental measurements of energetic charged particle fluxes in NES began in the early years of the space age [Vernov et al., 1958]. From these measurements, empirical models of ERB were developed in the 1970s and 80s. These models describe the spatial and energy distribution of omnidirectional fluxes of protons with energies from hundreds of keV to hundreds of MeV and electrons with energies from tens of keV to ~7–10 MeV in a large region of NES from ~250 km to geostationary and highly elliptical orbits. The most well-known models are AP8, AE8 (USA), and AP9/AE9 [Ginet et al., 2013] based on newer experimental data. SINP MSU has also developed ERB models [Kuznetsov et al., 2014], which formed the basis for domestic standards regulating methods of assessing radiation conditions of satellite flight.

However, these models are stationary. Variations in particle fluxes are reflected in them only by setting fluxes for minimum and maximum solar activity, whereas the corresponding fluxes differ only for some energies a maximum of several times. At the same time, real charged particle fluxes in the vicinity of Earth, even under geomagnetically quiet conditions, are subjected to fairly significant medium- and long-term variations associated with solar and geomagnetic activity, variations in the geomagnetic field and the density of the upper atmosphere. Also noteworthy are rapid variations in cosmic ray fluxes, which primarily include short-term (with characteristic times of less than a few seconds) variations in electron fluxes of sub-relativistic and relativistic energies (from hundreds of keV to ~10 MeV).

In order to construct an adequate dynamic pattern of three-dimensional distribution of energetic radiation fluxes in NES, we should consider their time variations, including short-term variations in high-energy electron fluxes. In this case, the central problem is to figure out whether the detected variations in particle fluxes result from spatial or temporal effects. This problem is difficult to resolve with a single spacecraft. This requires simultaneous measurements with several spacecraft, which can be implemented using a multi-satellite constellation. Such problems are most effectively solved by comparative analysis of data from several spacecraft operating in both close and significantly different orbits. Such a strategy may be implemented as follows:

1) Sequential passage of closely spaced satellites through the same region, which allows the most reliable separation of spatial and temporal effects;

2) Simultaneous measurements on different L shells needed to restore the dynamic pattern of distribution of the trapped particle flux in a wide range of orbits, which, in particular, allows us to observe a shift of ERB maximum during geomagnetic disturbances;

3) Simultaneous measurements at one altitude by instruments of the same type installed on several satellites shifted in longitude relative to each other, which allows us to assess the influence of the local time factor on the particle flux dynamics.

Some of these problems can be solved by grouping several simultaneously launched spacecraft with identical detectors; the others, by analyzing data from one or more nanosatellites together with data from a larger spacecraft equipped with a complex of instruments providing detailed measurements of particle fluxes, the electromagnetic field, and other magnetospheric plasma parameters. It seems that standard-format micro- and nanosatellites, including CubeSats, are the most suitable spacecraft for implementing the multi-satellite measurement strategy considered. Such satellites are relatively cheap and do not require complex development stages and special tests. As a rule, they are launched into orbit by the associated launch, which also considerably reduces the cost of the mission. At the same time, there is no need to completely duplicate the functionality of large spacecraft. The advantage of the micro- and nanosatellite constellation lies precisely in the possibility for examining in more detail the time variations of different cosmic radiation components in various NES regions [Caspi et al., 2022].

1. MULTI-SATELLITE MISSION SOZVEZDIE-270 OF MOSCOW UNIVERSITY

In recent years, Moscow State University has been implementing its own space program, which involves monitoring charged particle fluxes in NES, as well as solar X-rays and gamma rays — electromagnetic transients of different nature. Noteworthy in this regard is the successful launch of such satellites as Universitetskiy—Tatiana [Sadovnichy et al., 2011], Universitetskiy—Tatiana-2 [Sadovnichy et al., 2011], Vernov [Panasyuk et al., 2016a, b], and Lomonosov [Sadovnichii et al., 2017]. The next step in this direction is a new project of Moscow University Sozvezdie-270, which intends to deploy a constellation of nanosatellites. By the end of 2024, 20 CubeSat nanosatellites had been launched (starting in 2018), 9 of which continue to operate in polar orbit at a height of ~500 km. Among them is the Avion spacecraft, launched on June 27, 2023, which provided the maximum amount of scientific data.

At present, the satellite constellation, deployed under the Sozvezdie-270 project, operates in the monitoring mode for individual events, but in the future it is

expected to be expanded, as well as to create a network of receiving stations distributed along the meridians, which will allow us to quickly obtain large amount of data and thus to turn to monitoring of cosmic radiation in near real-time mode. At least five ground-based receiving stations should be deployed using antennas operating in VHF, S, and X bands in the regions from Kaliningrad to Kamchatka. As a result, a unified system consisting of space and ground segments will be developed. It should ensure spacecraft control, as well as regular data reception from the constellation's satellites located at different NES points, and will significantly increase the amount of transmitted information. The main purpose of the multi-satellite constellation is to monitor cosmic radiation and electromagnetic transients of atmospheric, astrophysical, and solar origin.

To conduct experiments with CubeSat satellites, various instruments have been developed for detecting energetic charged particles, hard X-rays and gamma rays, as well as optical (ultraviolet and red) airglow.

To date, measurements with the satellite constellation of Moscow University have provided important information about the effects associated with various manifestations of solar flare activity and its impact on geomagnetic conditions in NES. Among such phenomena is penetration of SCRs into the polar caps, which leads to a significant change in radiation fields in the inner magnetosphere. In this regard, an important part is also played by a change in the spatial structure of the distribution of high-energy electron fluxes in outer ERB due to magnetic storms, which, in turn, are caused by changes in IMF and SW parameters due to active processes on the Sun. Another direction in the study of radiation conditions in NES is to examine the dynamics of sub-relativistic electron fluxes in the regions of precipitation from inner (L~1.6÷1.8) and outer ERBs.

Bellow, we discuss examples of observations of these phenomena, made using mainly instruments on board Avion SC and some other satellites of Sozvezdie-270. There are three detector modules of the DeCoR type installed on board Avion SC: DeCoR-1, DeCoR-2, and DeCoR-3 [Bogomolov et al., 2020]. The DeCoR instruments are scintillation spectrometers that utilize a combination of a thin layer of plastic scintillator and a thicker CsI(Tl) crystal as a detector element. In front of the CsI(Tl) crystal is a thin layer of plastic scintillator, which simultaneously serves as a detector of charged particles (mostly electrons) and an active protection of the CsI(Tl) channel, which uses the separation of events in different scintillators by the shape of the light pulse at the output of the photodetectors. Hard X-rays is detected by CsI(Tl) scintillation crystals.

The detectors installed on Avion differ in the size of the sensitive region optimized for solving specific scientific problems. In particular, DeCoR-2 is optimized for recording and studying cosmic gamma-ray bursts of different nature. It has an effective area increased to ~65 cm^2, which is necessary to increase sensitivity and improve temporal resolution, determined primarily by the statistics of detected gamma-rays. The DeCoR-2 module is a composite scintillation detector (phoswich) consisting of a 3 mm plastic scintillator and a 9 mm CsI(Tl) crystal. Both scintillators are viewed by an assembly of silicon photomultipliers (SiPM), which ensures separate recording of gamma quanta and electrons in the energy release range in scintillators from 20 keV to 1 MeV. This separation is important when conducting an experiment to study gamma-ray bursts in a polar orbit.

In addition to DeCoR-2, two more detector modules are included in the equipment complex to ensure more accurate measurements. The DeCoR-1 module with scintillators having an area of ~18 cm^2, viewed by two vacuum photomultipliers (PMT), is designed to study changes in the electron flux in the energy release range from 50 keV to 2 MeV. It is completely analogous to the DeCoR instruments employed for the experiments carried out by VDNKh-80, Norby, Descartes, and other CubeSats [Bogomolov et al., 2020]. The DeCoR-3 module was added to expand the range of detected gamma rays to the high-energy range, i.e. up to 5 MeV. Its main purpose is to measure energy spectra of solar flare gamma rays and cosmic gamma-ray bursts. The detecting element of this unit is a CsI(Tl) scintillation crystal 30×30×30 mm^3, which is viewed by two vacuum PMT systems.

Data from each DeCoR module is recorded both as monitoring frames (count rate on several channels) and a detailed event-by-event record. The volume of scientific data transmitted from the Avion DeCoR instruments is ~5 MB per day. The main type of transmitted data is frames in monitoring mode with a time resolution of 1 s, and during the flight it is possible to repeatedly change this value, both up and down. The lower threshold for detecting quanta is several tens of keV, it can also be changed during flight, taking into account background conditions in near-Earth orbit, while the detectors can be configured differently.

The data from the CubeSat satellites of the MSU constellation, including the Avion spacecraft, are available in the form of graphs and tables on the SINP MSU space weather website [https://swx.sinp.msu.ru/tools/davisat.php].

2. EXAMPLES OF OBSERVATIONS OF SPACE WEATHER EFFECTS

2.1. Solar cosmic rays

As an example illustrating the possibilities of experiments on detection of SCR events by CubeSat nanosatellites, let us consider two increases in solar electron fluxes in the polar caps: the former began immediately after midnight on June 8, 2024; the latter, around midnight on June 12, 2024 (Figure 1). The top panel exhibits time dependences of count rates N of >300 keV electrons, obtained by DeCoR-1 and DeCoR-3 on board Avion SC (dark blue and purple dots respectively). Measurements are shown in the polar caps — regions of open field lines to which SCRs penetrate.

Circled marks (squares for DeCoR-1 and circles for DeCoR-3) represent measurements in the southern polar cap; uncircled marks, in the northern one. Curves of SCR electron fluxes are seen to be not completely identical

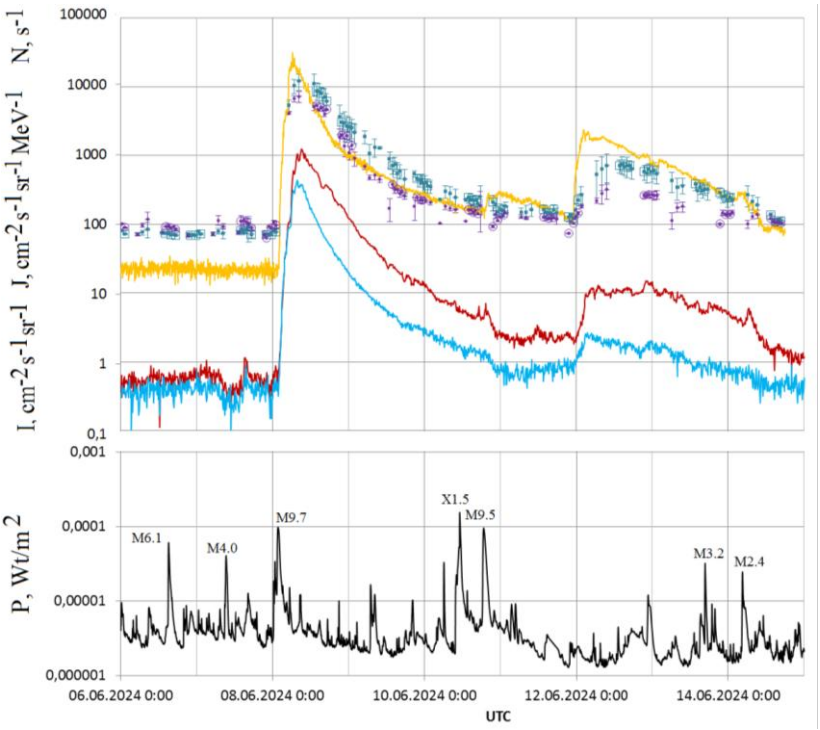

Figure 1. Time dependences (at the top) of count rates *N* of >300 keV electrons obtained by DeCoR-1 and DeCoR-3 on board Avion SC (dark blue and purple dots respectively; circled marks correspond to measurements in the southern polar cap; uncircled, in the northern one); time dependence of 175–315 keV electron flux *J* derived during an experiment on board ACE SC (yellow curve), and time dependences of proton fluxes *I* with an energy 9–20 MeV (red curve) and 20–40 MeV (blue curve), derived during an experiment on board Electro-L2 SC; at the bottom is the time dependence of X-ray fluxes from GOES data

in the northern and southern caps during this event, i.e. there is an asymmetry that may be linked both to anisotropy of the fluxes and to different orientations of the instruments relative to geomagnetic field lines. Simultaneously with Avion measurements, the top panel shows the time dependence of *J* electron flux with an energy 175–315 keV, obtained during an experiment on board ACE SC (yellow curve), and time dependences of *I* proton fluxes with an energy 9–20 MeV (red curve) and 20–40 MeV (blue curve), obtained by the SKIF instrument during an experiment on board Electro-L2 SC operating in geostationary orbit. The bottom panel displays the time dependence of X-ray fluxes from GOES-16 SC. The time dependences of SCR electron fluxes in the polar caps and at the L1 point are seen to be in fairly good agreement, as observed during earlier experiments [Kuznetsov et al., 2003]. Note that the possibility of obtaining data on SCR electron fluxes near Earth is an advantage of experiments in circular polar orbits since such data cannot be collected during experiments at geostationary orbit due to the fact that it is located in outer ERB.

The source of the first increase in SCRs (June 8 – June 10) was a solar flare of M9.8 class according to the GOES classification (see the bottom panel in Figure 1). The flare began on June 8, 2024 at 01:23 UT in active region (AR) AR13697, which was located in the southern hemisphere near the western limb (coordinates of the flare S18W69) during the flare. It was quite long — the soft X-ray emission maximum was recorded at 01:49 UT; the end of the flare, at 02:07 UT. The flare was accompanied by a coronal mass ejection (CME), which was recorded on June 8, 2024 at 01:48 UT. Figure 1 shows that the time dependences of SCR proton fluxes according to Electro-L2 data and SCR electron fluxes according to ACE and Avion data are similar, although not identical, and have a profile characteristic of SCR events from western flares — a rapid increase in SCR particle flux and a much longer gradual decrease. It can be seen that the increase in the solar proton flux according to Electro-L2 data began immediately after the soft X-ray burst at ~02:10 UT, the maximum proton flux caused by this event in the above range was detected on June 8 at 06:20 UT.

The second rather intense SCR event (see Figure 1) began on June 12, 2024 around midnight. Its source was a post-limb flare that probably occurred in AR13697 as the flare that triggered the above SCR event. This flare was also accompanied by halo-type CME with an initial velocity of ~2000 km/s, which was recorded on June 11, 2024 at 23:20 UT. As in the first SCR event considered, simultaneously with increases in SCR electron fluxes in the polar caps (Avion) and at L1 (ACE) on June 11–12, 2024 near midnight, the SKIF instrument installed on the Electro-L2 geostationary satellite also detected an increase, i.e. SCR protons and electrons arrived at Earth's orbit in both SCR events.

In conclusion of this section, we would like to note that, despite many years of observation of SCR events, the creation of SPE catalogs and theoretical models, some problems remain unresolved. So, even in the above short time period (see Figure 1), it is apparent

that neither the most intense X1.5 flare occurring in AR13697 during this period on June 10, 2024, nor the subsequent M9.5 class flare (again in the same AR) belong to significant SPEs comparable in amplitude to the two SCR events discussed above for protons and electrons. There is a need for further experimental studies of SCR events, which will be useful in developing theoretical and predictive models.

2.2. Dynamics of Earth's outer radiation belt during a magnetic storm

Another significant manifestation of space weather, which can also be monitored by CubeSat nanosatellites during experiments, is a change in outer ERB during magnetic storms. Let us take a closer look at the outer ERB dynamics, using Avion data for the period from August 11 to August 15, 2024, when there was fairly high geomagnetic activity.

Figure 2 plots time dependences of count rates of >300 keV electrons recorded by DeCoR-1 on board Avion SC (purple line, left scale) and the McIllwain parameter *L* (yellow line, right scale) for the time intervals on August 10, 2024 from 21:27 to 23:42, on August 12, 2024 from 21:15 to 23:30, and on August 14, 2024 from 21:03 to 23:18 UT before, during, and after the magnetic storm that began at the end of August 11, 2024. The given intervals are chosen in such a way as to exclude the longitude effect since for each of the three time intervals the spacecraft passes along the same longitudes.

The obtained time dependences of count rates of outer ERB electrons are seen to change with time.

Let us examine geomagnetic conditions of this time interval in more detail. A strong disturbance of IMF, probably caused by the arrival of an interplanetary coronal mass ejection (ICME) at Earth, which resulted from the merger of several, at least three, CMEs that left the Sun from August 8 to August 10, 2024. The maximum ejection velocity recorded by LASCO (SOHO) on August 8, 2024 at 19:48 UT was 789 km/s, the maximum SW velocity at Earth's orbit was ~520 km/s; and its maximum density, ~35 cm^{-3}.

The storm main phase began on August 11–12, 2024 around midnight. The maximum amplitude of *Dst* variation of ~–203 nT was observed on August 12 at 17:00, with maximum K_p being 8. The geomagnetic indices K_p and *Dst* for August 9–16, 2024 are shown in Figure 3. Colored arrows represent the time points when data on outer ERB was obtained (see Figure 4).

The left panel of Figure 4 plots *L* dependences of the measurement point proportional to the magnetic latitude, electron count rates before (blue line), during (red line), and after (green line) the August 11–12, 2024 magnetic disturbance for the time intervals (see arrows in Figure 3). In the right panel are maps with a projection of the Avion orbit onto Earth for observations presented in the left panels. The curves were obtained from observations for the following time intervals that correspond to the intersection of the satellite's orbit with ERB (see Figure 2), when the spacecraft moved from the polar region to the equator. The top panel presents data on August 10, 2024 at 21:46–22:10, August 12 at 21:31–21:55, and August 14 at 21:16–21:40 UT, i.e. in the Northern Hemisphere. The bottom panel displays data on August 10, 2024 at 22:30–23:00, on August 12, 2024 at 22:15–22:45, and on August 14 at 22:00–22:30 UT, i.e. in the Southern Hemisphere.

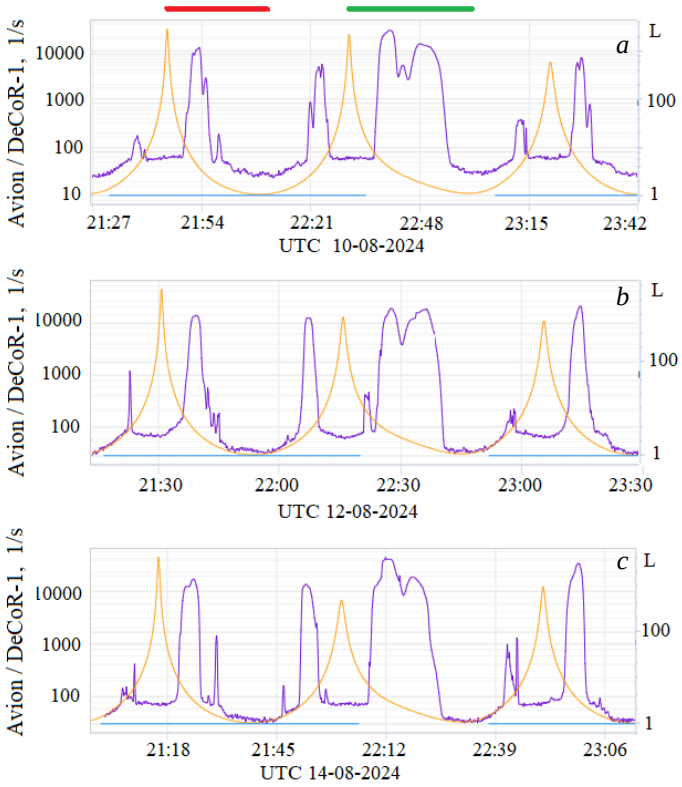

Figure 2. Time dependences of electron count rates by Avion DeCoR-1 (purple line, left scale) and the McIlvaine parameter L (yellow line, right scale) on August 10 (*a*), August 12 (*b*), and August 14, 2024 (*c*). Horizontal red and green lines indicate the time intervals used in Figure 4 (see below)

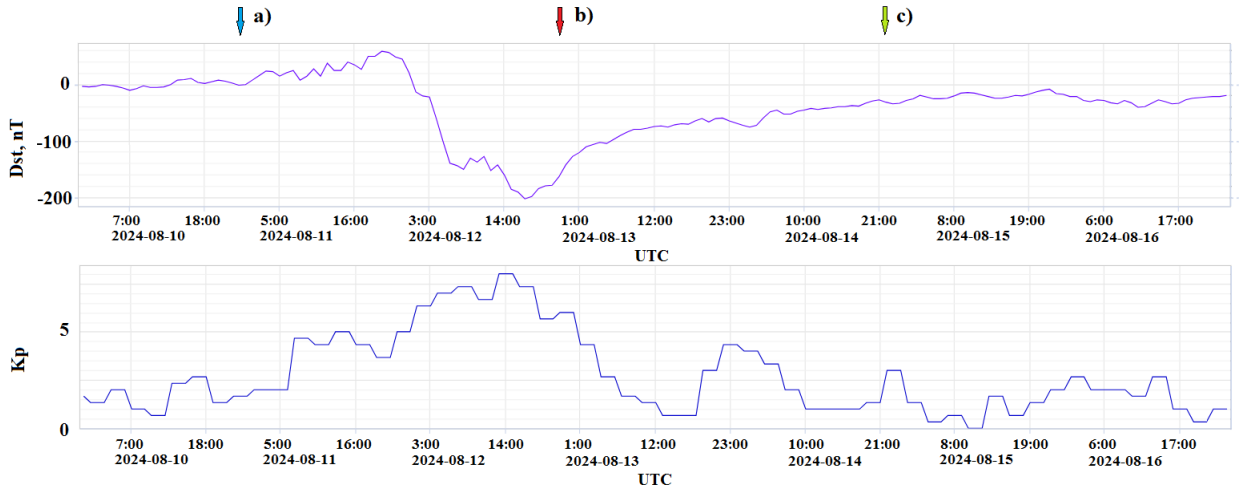

Figure 3. Time dependences of the geomagnetic activity indices *Dst* (top) and K_p (bottom). Arrows indicate measurement moments on the Avion spacecraft, shown in Figure 4

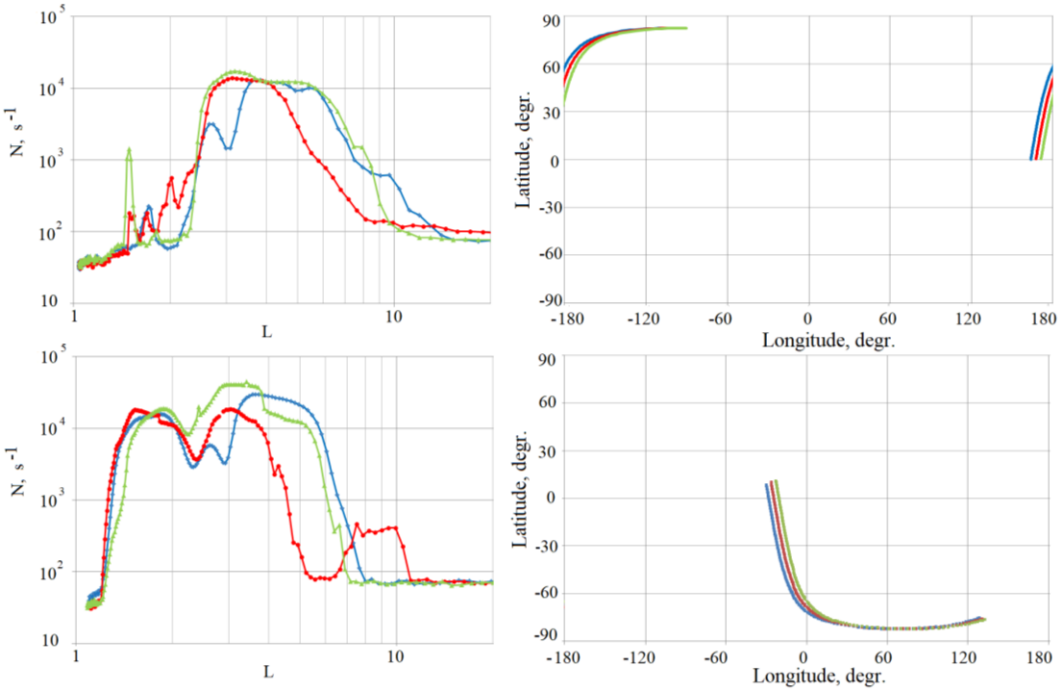

Figure 4. On the left: *L* dependences of electron count rates before (blue line), during (red line), and after (green line) the August 11–12, 2024 magnetic disturbance for the time intervals denoted in Figure 2 by the red line (top panel) and the green line (bottom panel). On the right: maps with a projection of the Avion orbit onto Earth for observations presented in the left panels

It can be observed that in the Northern Hemisphere at the maximum of the storm the intensity of outer ERB remained virtually unchanged, but its maximum shifted closer to Earth, from L=4 to L=3, where there was a gap between outer and inner belts before the storm. The high-latitude boundary of outer ERB also shifted to smaller L — from L~8÷9 to L~6÷7. In the Southern Hemisphere, at the maximum of the storm, the intensity of sub-relativistic electron fluxes decreased several times, the equatorial boundary, as in the Northern Hemisphere, shifted to smaller L, i.e. in both hemispheres, the gap was filled with particles. In the Southern Hemisphere, the polar boundary of outer ERB shifted from L~7÷8 to L~5÷6. Since the equatorial boundary of the outer belt shifted less in both hemispheres, it can be said that by the end of the storm main phase the outer belt seemed to compress. Also noteworthy in the Southern Hemisphere is an additional high-latitude increase in electron fluxes in the L region from 8 to 10. Clarifying the nature of such high-latitude increases requires further research.

At the end of the recovery phase (on August 14), the high-latitude boundary of outer ERB returned to the pre-storm level in both hemispheres. In the Southern Hemisphere, the intensity at the maximum, which remained closer to Earth than before the storm, increased. The polar boundary of outer ERB returned to the pre-storm level in both hemispheres, the pre-storm gap region remained filled with particles, i.e. the space filled with electrons of outer ERB under the action of the geomagnetic storm increased in this case, as was repeatedly observed during other experiments (e.g., [Myagkova et al., 2021]).

2.3. Electron precipitation from the inner belt

The third problem in terms of space weather phenomena is the study of variations of precipitation from inner ERB. As an example, let us examine variations in the electron count rate in the region of precipitation from inner ERB (L~1.6÷1.8). Before the magnetic storm, there was one peak of intensity at L~1.7 (blue curve in Figure 4). Two additional peaks appeared during the storm, at L~1.6 and L~2 (red curve in Figure 4). After the end of the storm, the amplitude of the peak at L~1.6 increased significantly after its end (green curve in Figure 4). Note that the peaks near 1.6 were observed on August 12 at ~21:44 and on August 14 at ~21:30 UT, i.e. approximately at the same time. Thus, the question arises whether the dynamics of the count rate of sub-relativistic electrons precipitating from inner ERB at L~1.6 is related to geomagnetic activity or there are other factors.

To answer this question, we analyzed Avion measurements made during the August 8, 2024 magnetic storm and during the quiet period on September 25 – October 3, 2024. Time dependences of the count rate of >300 keV electrons derived from measurements performed by Avion with the aid of DeCoR-1 are shown in Figure 5. We also analyzed data from the Altair CubeSat, obtained on December 13, 2024, also during the magnetically quiet period.

A map of the Avion and Altair CubeSats' orbits projected onto Earth for these measurements is presented in Figure 6. Since the spacecrafts' orbits are close to sun-synchronous, they pass through the same regions at approximately the same UT. Circles mark regions where sub-relativistic electrons precipitated from inner ERB.

The L dependences of >300 keV electron count rates, obtained using the Avion and Altair CubeSats (see trajectories in Figure 6), are plotted in Figure 7. The green line indicates Avion spacecraft data received on August 14,

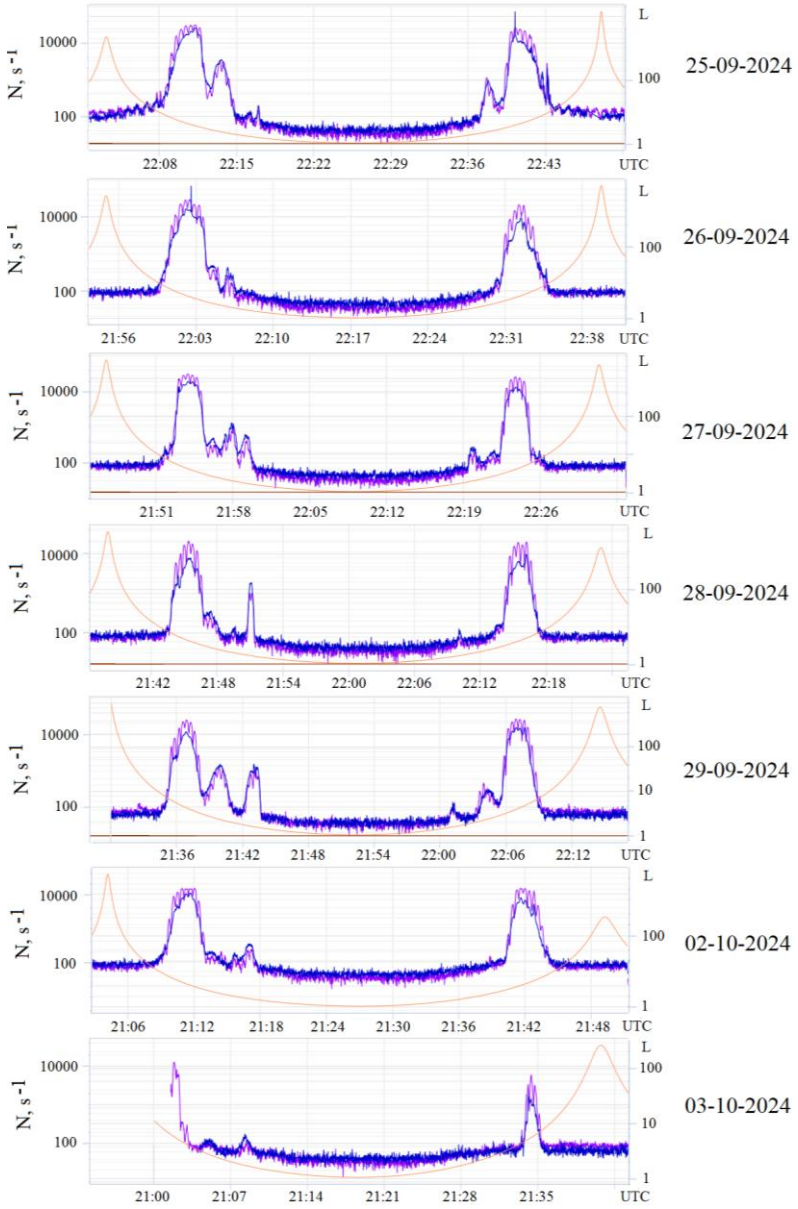

Figure 5. Time dependences of count rates of electrons from Avion DeCoR-1 (purple line, left scale) and DeCoR-3 (blue line, left scale), as well as the McIllwain parameter L (orange line, right scale) for magnetically quiet periods

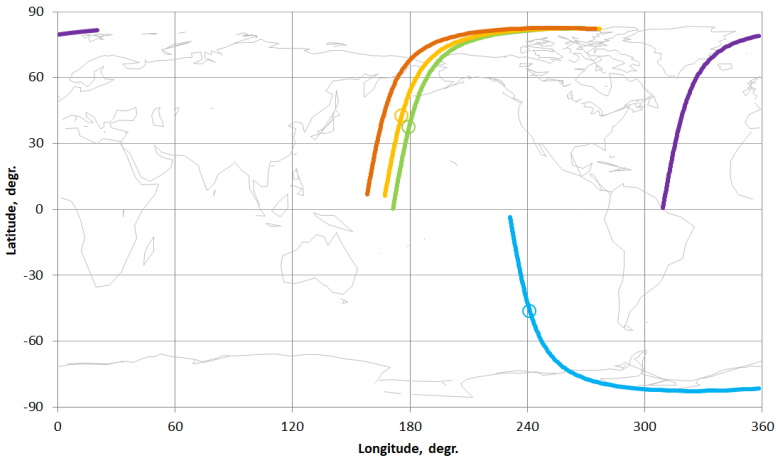

Figure 6. Map with a projection of the Avion and Altair CubeSats's orbits onto Earth: the green line is the Avion orbit on August 14, 2024 at 21:16–21:40; the yellow line is the Avion orbit on September 28, 2024 at 21:38–22:00; the purple line is the Avion orbit on September 28, 2024 at 12:06–12:30; orange line, the Altair orbit on December 13, 2024 at 09:48–10:11; blue line, the Altair orbit on December 13, 2024 at 16:53–17:17 UT. Circles mark the regions where sub-relativistic electrons precipitate from the inner belt

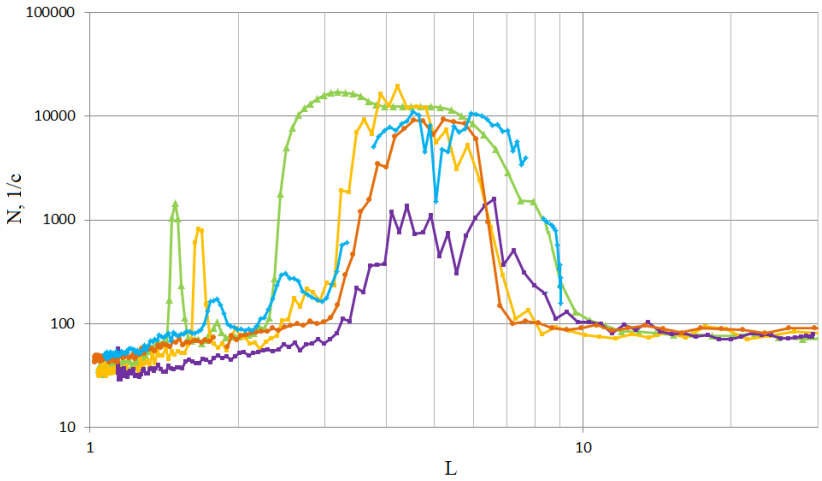

Figure 7. Dependences of electron counting rates on *L*, obtained on the Avion and Altair CubeSats for the measurements shown in Figures 5 and 6. The green line is Avion on August 14, 2024 at 21:16–21:40 UT (after the magnetic storm); the yellow line is Avion on September 28, 2024 at 21:38–22:00 UT (similar orbit and UT); the purple line, Avion on September 28, 2024 at 12:06–12:30 UT (different orbit and UT); the red line, Altair on December 13, 2024 at 09:48–10:11 UT (similar orbit, different UT); the blue line, Altair on December 13, 2024 at 16:53–17:17 UT (different orbit, similar UT)

2024 at 21:16–21:40 UT (after the magnetic storm that began on August 11, 2024); the yellow line (Avion), on September 28, 2024 at 21:38–22:00 UT (similar orbit and UT, *Dst*=–11 nT, K_p=2+); the purple line (Avion), on September 28, 2024 at 12:06–12:30 UT (different orbit and UT, *Dst*=3 nT, K_p=2–); the red line (Altair), on December 13, 2024 at 09:48–10:11 UT (similar orbit, different UT, *Dst*=1 nT, K_p=1+); the blue line (Altair), on December 13, 2024 at 16:53–17:17 UT (different orbit, similar UT, *Dst*=–6 nT, K_p=1+).

The above Figures show that in the regions under study (at *L*~1.7) there were short-term sharp increases (peaks) in >300 keV electron fluxes both before the onset of the magnetic storm (August 10), during the magnetic storm (August 12), and during the magnetically quiet period in December 2024 (data from the Altair CubeSat). At the same time, during the magnetic storm in August, another peak appeared at *L*~1.6, which reached a much higher amplitude on August 14, and the peak at *L*~1.7 ceased to be observed. Combination of these facts suggests that the August 11–12, 2024 geomagnetic storm was so strong that it caused a disturbance not only in outer ERB, but also in the inner one, which led to a change in the distribution of sub-relativistic electron fluxes in the precipitation region.

If we consider this region as a whole, i.e. from *L*~1.6÷1.9, it should be noted that sharp increases in sub-relativistic electron fluxes on these *L* shells can occur in the region of 180° E both during magnetic storms and during magnetically quiet periods, and reach maximum values in the evening (UT).

In order to determine whether the observed intensity maxima of precipitating electrons are due to certain UT or reflect the spatial distribution of fluxes on certain drift shells or in certain geographic regions, we analyzed measurements at orbits intersecting the shells *L*~1.6÷1.9 at other longitudes (purple curve in Figures 6, 7).

Figure 7 shows that at ~320°–330° longitudes around noon (UT) there were no increases in intensity at *L*~1.6÷1.7, which allows us to conclude that precipita-

tion at these longitudes is probably linked either to a certain geographic region or to a certain UT interval.

To analyze both possibilities, we have compared electron count rates measured when different spacecraft passed through the same region, crossing it at different points (UT). To do this, in addition to Avion data, Figures 6, 7 plot two more trajectories and two additional sub-relativistic electron count rate profiles as function of L (red and blue lines). They were obtained from measurements made by DeCoR-2 (it also measured the count rates of >300 keV electrons) on board the Altair CubeSat, whose orbit is analogous to that of Avion. The red curve in Figure 7 represents the L dependence of electron flux, measured when Altair crossed the same region at L~1.6 as Avion, but much earlier (09:48–10:11 UT). In this case, the electron flux did not increase at L<2. However, a peak at L~1.8 was detected during other Altair passes, the L dependence for one of which is indicated by the blue line in Figure 7. At that time (16:53–17:17 UT), Altair moved from the southern polar cap to the equator over the Pacific Ocean. These results allow us to conclude that significant peaks at L~1.6÷1.9 are observed in different geographic regions, but during certain periods (UT), i.e. mainly in the afternoon and evening.

Note that significant fluxes of sub-relativistic electrons at L~1.6÷1.9 were previously detected by the OHZORA [Nagata et al., 1988], CORONAS-I satellites [Bashkirov et al., 1999; Kuznetsov, Myagkova, 2001; Kuznetsov, Myagkova, 2002], and the Mir orbital station [Bogomolov et al., 2005]. In particular, Kuznetsov, Myagkova [2002] have shown that electrons at L~1.6 are generally recorded at longitudes 110°–200°, 200°–290° from 10 to 24 UT. Kuznetsov and Myagkova [2002] conclude that precipitation at L~1.6 may be caused by thunderstorm activity, yet it is not unlikely that the precipitation may be linked to variations in the geomagnetic activity indices. We can say that the results of measurements of sub-relativistic electron fluxes at L~1.6÷1.9 with the Moscow University SC constellation do not contradict these conclusions.

CONCLUSION

In this paper, we have provided examples of observation of some space weather phenomena during experiments conducted with instruments developed at SINP MSU and installed on CubeSats of the Sozvezdie-270 constellation. In particular, we have demonstrated possibilities of measuring solar electron fluxes in NES for SCR events, have carried out observations of filling of the polar caps with SCR particles, which were used to obtain time dependences of the average count rate of sub-relativistic electrons in the polar caps during the June 8–10 and 12–14, 2024 SCR events. These dependences agree well with time variations of SCR electron fluxes at the L1 libration point, which were measured by ACE, as well as with the SCR proton profile from Electro-L2 data. We also acquired data on the dynamics of spatial distributions of sub-relativistic electron fluxes in outer ERB during the August 11–12, 2024 strong magnetic storm, which showed that during the magnetic storm main phase the outer ERB region seemed to compress. This is due to the smaller shift in the equatorial boundary of the belt (to the region of the pre-storm location of the gap) as compared to the more noticeable shift in the polar boundary of ERB. During the recovery phase, the polar boundary returns to the position observed before the storm, whereas the equatorial boundary continues to remain close to Earth, due to which the region occupied by sub-relativistic electrons of outer ERB expands.

Also noteworthy are the results of studies into the dynamics of fluxes of sub-relativistic electrons precipitating from inner ERB at L~1.6÷1.8. We have shown that significant fluxes on these drift shells are generally observed in different geographic regions during a certain UT period at different geomagnetic activity levels. At the same time, in the case of the severe magnetic storm on August 11, 12, 2024, the spatial distribution of electron fluxes in the precipitation region underwent some variations. The results do not contradict the conclusions drawn earlier from OHZORA and CORONAS-I observations. Particularly noteworthy is that observations from different satellites of the Moscow University multi-satellite constellation Sozvezdie-270 have been used for the first time to obtain a more complete picture of the dynamics and spatial structure of precipitating electrons. Naturally, in order to draw certain conclusions on the dynamics and mechanisms of sub-relativistic electron precipitation from inner ERB, further research is needed to which satellite measurements can make a significant contribution. In this regard, the role of Sozvezdie-270 is very important.

The work was financially supported by Research and Educational School of M.V. Lomonosov Moscow State University "Fundamental and Applied Space Research", project No. 24-Sh01-05 Sozvezdie-270. It was carried out under Government assignment of M.V. Lomonosov Moscow State University.

REFERENCES

Baker D.N. Satellite anomalies due to space storms. *Space Storms and Space Weather Hazards*. 2001, vol. 38. Springer, Dordrecht. DOI: 10.1007/978-94-010-0983-6_11.

Bashkirov V.F., Denisov Y.I., Gotselyuk Y.V., et al. Trapped and quasi-trapped radiation observed by “CORONAS-I” satellite. *Radiation Measurements*. 1999, vol. 30, no. 5, pp. 537–546.

Belov A.V., Villoresi J., Dorman L.I., M.I. et al. Effect of the space on operation of satellites. *Geomagnetism and Aeronomy*. 2004, vol. 44, no. 4, pp. 461–468.

Bogomolov A.V., Denisov Y.I., Kolesov G.Y., et al. Fluxes of quasi-trapped electrons with energies >0.08 MeV in the near-earth space on drift shells L<2. *Cosmic Res.* 2005, vol. 43, no. 5, pp. 307–313.

Bogomolov V.V., Bogomolov A.V., Dement’ev Yu.N., Eremeev V.E., et al. A first experience of space radiation monitoring in the multi-satellite experiment of Moscow University in the framework of the Universat-SOCRAT project. Moscow University *Physics Bulletin*. 2020, vol. 73, no. 6, pp. 676–683. DOI: 10.3103/S0027134920060089.

Caspi A., Barthelemy M., Bussy-Virat C.D., et al. Small satellite mission concepts for space weather research and as pathfinders for operations. *Space Weather*, 2022, vol. 20, iss. 2, e2020SW002554. DOI: 10.1029/2020SW002554.

Cole D.G. Space weather: Its effects and predictability. *Space Sci. Rev.* 2003, vol. 107, pp. 295–302.

DOI: 10.1023/A:1025500513499.
Daglis I.A. *Space Storms and Space Weather Hazards*. Kluwer, Dordrecht, Boston, 2001. DOI: 10.1007/978-94-010-0983-6.
Dorman L.I., Miroshnichenko L.I. *Solar Cosmic Rays*. Moscow: Nauka, 1968, 468 p. (In Russian).
Ginet G.P., O'Brien T.P., Huston S.L. AE9, AP9 and SPM: New models for specifying the trapped energetic particle and space plasma environment. *Space Sci. Rev*. 2013, vol. 179, pp. 579–615 DOI: 10.1007/s11214-013-9964y.
Iucci N., Levitin A., Belov E., Eroshenko E.A. Space weather conditions and spacecraft anomalies in different orbits. *Space Weather*. 2005, vol. 3, S01001. DOI: 10.1029/2003SW000056.
Kudela K. Space weather near Earth and energetic particles: selected results. *Journal of Physics: Conf. Series*. 2013, vol. 409, iss. 1, article id. 012017. DOI: 10.1088/1742-6596/409/1/012017.
Kuznetsov S.N., Myagkova I.N. Fluxes of quasi-trapped particles under the Earth's radiation belts. *Geomagnetism and Aeronomy*. 2001, vol. 41, no. 1, pp. 10–13.
Kuznetsov S.N., Myagkova I.N. Quasi-trapped electron fluxes (>0.5 MeV) under the radiation belts: analysis of their connection with geomagnetic indices. *J. Atmos. Solar-Terr. Phys*. 2002, vol. 64, no. 5-6. pp. 601–605.
Kuznetsov S.N., Bogomolov A.V., Denisov Y.I., et al. The solar flare of November 4, 2001, and its manifestations in energetic particles from CORONAS-F data. *Solar System Res*. 2003, vol. 37, pp. 121–127. DOI: 10.1023/A:1023384425209.
Kuznetsov N.V., Nymmik R.A., Panasyuk M.I., Popova E. Working model of flows of space charged particles and new experimental data. *Voprosy atomnoi nauki i tekhniki* [Problems of Atomic Science and Technology. Ser. Physics of Radiation Effects…] 2014, no. 1, pp. 44–48. (In Russian).
Lundstedt H. The Sun, space weather and GIC effects in Sweden. *Adv. Space Res*. 2006, vol. 37, no. 6, pp. 1182–1191. DOI: 10.1016/j.asr.2005.10.023.
McGranaghan R.M., Camporeale E., Georgoulis M., Anastasiadis A. Space weather research in the digital age and across the full data lifecycle: Introduction to the topical issue. *J. Space Weather and Space Climate*. 2021, vol. 11, p. 50. DOI: 10.1051/swsc/2021037.
Myagkova I.N., Bogomolov A.V., Eremeev V.E., et al. Dynamics of the Radiation Environment in the Near-Earth space in September–November 2020 according to the Meteor-M and Electro-L Satellite Data. *Cosmic Res*. 2021, vol. 59, iss. 6, pp. 433–445. DOI: 10.1134/S0010952521060071.
Nagata K., Kohno T., Murakami H., Nakamoto A., Hasebe N., Kikuchi J., Doke T. Electron (0.19–3.2 MeV) and proton (0.58–35 MeV) precipitations observed by OHZORA satellite at low latitude zones L=1.6–1.8. *Planet. Space Sci*. 1988, vol. 36, pp. 591–606.
Novikov L.S., Voronina E.N. Interaction of spacecraft with the environment. Moscow: KDU, 2021.
Panasyuk M.I., Svertilov S.I., Bogomolov V.V., et al. Experiment on the Vernov satellite: Transient energetic processes in the Earth atmosphere and magnetosphere. Pt 1. Description of the experiment. *Cosmic Res*. 2016a, vol. 54, no. 4, pp. 261–269. DOI: 10.1134/S0010952516040043.
Panasyuk M.I., Svertilov S.I., Bogomolov V.V., et al. Experiment on-the Vernov satellite: Transient energetic processes in the Earth atmosphere and magnetosphere. Pt 2. First results. *Cosmic Res*. 2016b, vol. 54, no. 5, pp. 343–350. DOI: 10.1134/S0010952516050051.
Potapov A., Ryzhakova L., Tsegmed B. A new approach to predict and estimate enhancements of "killer" electron flux at geosynchronous orbit. *Acta Astronaut.* 2016, vol. 126, pp. 47–51. DOI: 10.1016/j.actaastro.2016.04.017.
Romanova N.V., Pilipenko V.A., Yagova N.V., et al. Statistical correlation of the rate of failures on geosynchronous satellites with fluxes of energetic electrons and protons. *Cosmic Res.* 2005, vol. 43, pp. 179–185. DOI: 10.1007/s10604-005-0032-6.
Sadovnichii V.A., Panasyuk M.I., Yashin I.V., et al. Investigations of the space environment aboard the Universitetsky-Tat'yana and Universitetsky—Tat'yana-2 microsatellites. *Solar System Res*. 2011, vol. 45, no. 1, pp. 3–29.
Sadovnichii V.A., Panasyuk M.I., Amelyushkin A.M., et al. "Lomonosov" satellite — space observatory to study extreme phenomena in space. *Space Sci. Rev*. 2017, vol. 212, no. 3-4. pp. 1705–1738. DOI: 10.1007/s11214-017-0425-x.
Schrijver C.J., Kauristie K., Aylward A.D., et al. Understanding space weather to shield society: A global road map 772 for 2015–2025 commissioned by COSPAR and ILWS. *Adv. Space Res.* 2015, vol. 55, pp. 2745–2807. DOI: 10.1016/j.asr.2015.03.023.
Vernov S.N., Grigorov N.L., Logachev YU.I., Chudakov A.Ye. Changes in cosmic radiation on an artificial Earth satellite. *Doklady Akademii Nauk*. 1958, vol. 120, no. 6, pp. 1231–1233. (In Russian).
Wei F., Feng X., Guo J.S., Fan, Q., Wu, J. Space weather research in China. *Adv. in Space Environment Res.* Springer, Dordrecht. 2003, pp. 327–334. DOI: 10.1007/978-94-007-1069-6_31.
Wilkinson P. Space weather studies in Australia. *Space Weather: The Intern. J. Research and Applications*. 2009, vol. 7, S06002. DOI: 10.1029/2009SW000485.
URL: https://swx.sinp.msu.ru/tools/davisat.php/ (accessed July, 22, 2025).

The 15th Russian-Chinese Space Weather Conference, September 9–13, 2024, Institute of Solar-Terrestrial Physics SB RAS, Irkutsk, Russia.

Original Russian version: Bogomolov A.V., Bogomolov V.V., Iyudin A.F., Kalegaev V.V., Myagkova I.N., Osedlo V.I., Svertilov S.I., Yashin I.V., published in Solnechno-zemnaya fizika. 2025, vol. 11, no. 3, pp. 137–148. DOI: 10.12737/szf-113202515.

How to cite this article

Bogomolov A.V., Bogomolov V.V., Iyudin A.F., Kalegaev V.V., Myagkova I.N., Osedlo V.I., Svertilov S.I., Yashin I.V. Monitoring of space weather effects with Sozvezdie-270 nanosatellite constellation of Moscow University. *Sol.-Terr. Phys*. 2025, vol. 11, iss. 3, pp. 125–134. DOI: 10.12737/stp-113202515.